Inorg. Chem. **2004**, *43*, 7196–7209

Reactivity of a (μ-Oxo)(μ-hydroxo)diiron(III) Diamond Core with Water, Urea, Substituted Ureas, and Acetamide

Sonia Taktak, Sergey V. Kryatov, and Elena V. Rybak-Akimova*

Department of Chemistry, Tufts University, Medford, Massachusetts 02155

Received May 13, 2004

A series of iron(III) complexes of the tetradentate ligand BPMEN (*N*,*N*′-dimethyl-*N*,*N*′-bis(2-pyridylmethyl)ethane-1,2-diamine) were prepared and structurally characterized. Complex $[Fe_2(\mu\text{-}O)(\mu\text{-}OH)(BPMEN)_2](ClO_4)_3$ (**1**) contains a (μ-oxo)(μ-hydroxo)diiron(III) diamond core. Complex $[Fe(BPMEN)(urea)(OEt)](ClO_4)_2$ (**2**) is a rare example of a mononuclear non-heme iron(III) alkoxide complex. Complexes $[Fe_2(\mu\text{-}O)(\mu\text{-}OC(NH_2)NH)(BPMEN)_2](ClO_4)_3$ (**3**) and $[Fe_2(\mu\text{-}O)(\mu\text{-}OC(NHMe)NH)(BPMEN)_2](ClO_4)_3$ (**4**) feature N,O-bridging deprotonated urea ligands. The kinetics and equilibrium of the reactions of **1** with ligands L (L = water, urea, 1-methylurea, 1,1-dimethylurea, 1,3-dimethylurea, 1,1,3,3-tetramethylurea, and acetamide) in acetonitrile solutions were studied by stopped-flow UV–vis spectrophotometry, NMR, and mass spectrometry. All these ligands react with **1** in a rapid equilibrium, opening the four-membered $Fe^{III}(\mu\text{-}O)(\mu\text{-}OH)Fe^{III}$ core and forming intermediates with a $(HO)Fe^{III}(\mu\text{-}O)Fe^{III}(L)$ core. The entropy and enthalpy for urea binding through oxygen are $\Delta H^\circ = -25$ kJ mol^{-1} and $\Delta S^\circ = -53.4$ J mol^{-1} K^{-1} with an equilibrium constant of $K_1 = 37$ L mol^{-1} at 25 °C. Addition of methyl groups on one of the urea nitrogen did not affect this reaction, but the addition of methyl groups on both nitrogens considerably decreased the value of K_1. An opening of the hydroxo bridge in the diamond core complex $[Fe_2(\mu\text{-}O)(\mu\text{-}OH)(BPMEN)_2]$ is a rapid associative process, with activation enthalpy of about 60 kJ mol^{-1} and activation entropies ranging from –25 to –43 J mol^{-1} K^{-1}. For the incoming ligands with the $-CONH_2$ functionality (urea, 1-methylurea, 1,1-dimethylurea, and acetamide), a second, slow step occurs, leading to the formation of stable N,O-coordinated amidate diiron(III) species such as **3** and **4**. The rate of this ring-closure reaction is controlled by the steric bulk of the incoming ligand and by the acidity of the amide group.

Introduction

Enzymes containing dinuclear metal centers in their active sites perform numerous essential biological functions ranging from oxygen transport to protein hydrolysis.[1–4] A significant number of these enzymes have been structurally characterized, revealing two proximate metal ions bridged by water ligands (O^{2-}, OH^-, or H_2O) and/or carboxylate groups from glutamate or aspartate residues.[1–4] Ligand exchange plays an important role in the function of metalloenzymes. Mammalian purple acid phosphatases are believed to use a diiron ($Fe^{II}Fe^{III}$) active site to hydrolyze phosphate esters by coordinating the substrate, attacking it by a hydroxide ligand, and then dispensing of the resulting phosphate by the exchange for water.[2–4] Significant ligand change occurs at the diiron site of soluble methane monooxygenase (sMMO) during its catalytic cycle in addition to redox transformations, and a high valent $Fe^{IV}(\mu\text{-}O)_2Fe^{IV}$ diamond core structure was proposed for one of the sMMO intermediates (Q).[5,6] Urease, which catalyzes the hydrolysis of urea, has two nickel(II) ions at its active site bridged by a hydroxide ion and by the carbamate from a modified lysine residue.[7,8] A probable mechanism for urease implies that urea coordinates to one nickel ion through its carbonyl oxygen, followed by a transition toward an N,O-bridging binding mode prior to or

* To whom correspondence should be addressed. E-mail: elena.rybak-akimova@tufts.edu.

(1) Kurtz, D. M., Jr. *J. Biol. Inorg. Chem.* **1997**, *2*, 159−167.
(2) Wilkox, D. E. *Chem. Rev.* **1996**, *96*, 2435−2458.
(3) Sträter, N.; Lipscomb, W. N.; Klabunde, T.; Krebs, B. *Angew. Chem., Int. Ed. Engl.* **1996**, *35*, 2024−2055.
(4) Averill, B. A. In *Comprehensive Coordination Chemistry II*; McCleverty, J. A., Meyer, T. J., Eds.; Elsevier: Amsterdam, 2004; Vol. 8, pp 641−676.
(5) Lipscomb, J. D.; Que, L., Jr. *J. Biol. Inorg. Chem.* **1998**, *3*, 331−336.
(6) Merkx, M.; Kopp, D. A.; Sazinsky, M. H.; Blazyk, J. L.; Muller, J.; Lippard, S. J. *Angew. Chem., Int. Ed.* **2001**, *40*, 2782−2807.
(7) Todd, M. J.; Hausinger, R. P. *Biochemistry* **2000**, *39*, 5389−5396.
(8) Benini, S.; Rypniewski, W. R.; Wilson, K. S.; Miletti, S.; Ciurli, S. *J. Biol. Inorg. Chem.* **2001**, *6*, 778−790.

10.1021/ic049371x CCC: $27.50
Published on Web 10/02/2004

Scheme 1

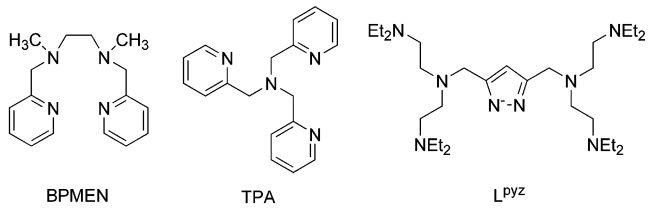

during hydrolysis.[8] In all cases, the enzyme active site interconverts during the catalytic cycle, and the nature of the bridging and terminal ligands around the metals varies.

In recent years, a wide variety of dinuclear metal complexes have been developed as structural and functional models of these enzymes' active sites.[9−12] In particular, doubly bridged oxo and/or hydroxo diiron complexes with neutral tetradentate aminopyridine ligands have emerged as an important class of structural models for compound Q of sMMO and other similar natural catalytic intermediates.[13−15] However, very little is known about the mechanism of small molecule addition and/or substitution at these diamond cores, which is essential to the fundamental understanding of their reactivity. There have been only a few kinetic studies on ligand substitution at dinuclear iron complexes.[16−21]

In this work, we used urea as a probe to study ring-opening and ring-closure processes at the Fe^{III}(μ-O)(μ-OH)Fe^{III} core in complex [Fe$_2$(μ-O)(μ-OH)(BPMEN)$_2$](ClO$_4$)$_3$ (**1**), where BPMEN is *N*,*N*′-dimethyl-*N*,*N*′-bis(2-pyridylmethyl)ethane-1,2-diamine (Scheme 1). Complex **1** has been characterized in solution and proposed to contain a (μ-oxo)(μ-hydroxo)-diiron(III) diamond core.[22−24] It was reported that **1** undergoes reversible hydration to yield a species with the (H$_2$O)Fe^{III}(μ-O)Fe^{III}(OH) core[23,24] and that **1** can react with some ligands in the protonated form HL (HSO$_4^-$, HOAc, HCO$_3^-$) to yield respective [Fe$_2$(μ-O)(μ-L)(BPMEN)$_2$]$^{n+}$ species.[22] Earlier, we reported kinetic and equilibrium studies of urea binding to a diiron(III) complex of TPA and to a pyrazolate-based dinickel(II) complex of L^{pyz} (Scheme 1).[20,25] In both cases, the first step of urea binding was very fast and a dinuclear species (HO)M···M(OC(NH$_2$)$_2$) with an O-bonded urea was proposed as the intermediate before ring closure and formation of the stable N,O-coordinated ureate dinuclear species M(μ-OC(NH$_2$)NH)M. In the BPMEN system, reaction rates were found to be slower, allowing for a better characterization of the O-bonded urea diiron intermediate using in situ electrospray mass spectrometry and electronic spectroscopy, as well as a more detailed kinetic study of this first binding step. Electronic and steric effects were also investigated by replacing urea with a series of *N*-methyl-substituted ureas, water, and acetamide.

Experimental Section

General Considerations. All reagents were obtained from commercially available sources and used without further purification, unless otherwise noted. Urea and 1,1,3,3-tetramethylurea were purchased from Acros. 1-Methylurea, 1,1-dimethylurea, 1,3-dimethylurea, and acetamide were purchased from Aldrich. Urea was recrystallized three times from hot water and dried overnight in the oven at 70 °C before use. The ligand BPMEN was synthesized according to a published procedure.[23] Infrared spectra of solids were recorded, in KBr pellets, on a Mattson RS-1 FTIR spectrometer and NMR spectra on a Bruker DPX-300 spectrometer. UV−vis spectra were acquired on a Hitachi U-2000 spectrophotometer or on a JASCO V-570 spectrophotometer. UV−vis spectra of solids were obtained in absorbance mode from Nujol mulls deposited on filter paper as described elsewhere[26] or by measurement of diffuse reflectance of pure solid sample. In situ electrospray mass spectra were obtained on a Finnigan LTQ mass spectrometer in positive ion detection mode. Electrospray tandem mass spectra were recorded by Agilent Technologies (Andover, MA) in positive ion detection mode. FAB mass spectra were collected by the mass spectrometry service laboratory at the University of Minnesota (Minneapolis, MN). Elemental analyses were performed by Desert Analytics (Tucson, AZ). **CAUTION:** Although no problems were encountered in this study, perchlorate salts of metal complexes with organic ligands are potentially explosive and should be handled with care!

[Fe$_2$(μ-O)(μ-OH)(BPMEN)$_2$](ClO$_4$)$_3$ (1). BPMEN (1.64 g, 6.07 mmol) was dissolved in 75 mL of ethanol/water (1:1 v/v) with sodium hydroxide (0.30 g, 7.50 mmol) and slowly added to a solution of Fe(ClO$_4$)$_3$·6H$_2$O (3.91 g, 7.62 mmol) dissolved in 15 mL of ethanol. The mixture was left overnight in the refrigerator. Different batches led to the formation of green crystals of [Fe$_2$(μ-O)(OH)(OH$_2$)(BPMEN)$_2$](ClO$_4$)$_3$·H$_2$O (**1a**) or a maroon powder (mixture of **1** and **1a**). Recrystallization of either of the solids from anhydrous acetonitrile gave pure complex **1**. In a typical procedure, green solid **1a** (20 mg, 0.02 mmol) was dissolved in 1 mL of dry acetonitrile under argon atmosphere and the solvent was allowed to slowly evaporate. Red crystals suitable for X-ray diffraction analysis were obtained after 2 weeks. Yield: 17 mg (86%). UV−vis (400−800 nm, reflectance of pure solid): λ_{max} 430(sh), 477-(sh), 512(sh), 555. Anal. Calcd (found) for C$_{32}$H$_{45}$N$_8$Fe$_2$Cl$_3$O$_{14}$: C, 39.07 (38.39); H, 4.61 (4.29); N, 11.39 (11.26).

(9) Gavrilova, A. L.; Bosnich, B. *Chem. Rev.* **2004**, *104*, 349−384.
(10) Tshuva, E. Y.; Lippard, S. J. *Chem. Rev.* **2004**, *104*, 987−1012.
(11) Fontecave, M.; Ménage, S.; Duboc-Toia, C. *Coord. Chem. Rev.* **1998**, *178*−*180*, 1555−1572.
(12) Than, R.; Feldman, A. A.; Krebs, B. *Coord. Chem. Rev.* **1999**, *182*, 211−241.
(13) Que, L., Jr.; Tolman, W. B. *Angew. Chem., Int. Ed.* **2002**, *41*, 1114−1137.
(14) Costas, M.; Rohde, J.-U.; Stubna, A.; Ho, R. Y. N.; Quaroni, L.; Münck, E.; Que, L., Jr. *J. Am. Chem. Soc.* **2001**, *123*, 12931−12932.
(15) Egdal, R. K.; Hazell, R.; Larsen, F. B.; McKenzie, C. J.; Scarrow, R. C. *J. Am. Chem. Soc.* **2003**, *125*, 32−33.
(16) Drüeke, S.; Wieghardt, K.; Nuber, B.; Weiss, J.; Fleischhauer, H.-P.; Gehring, S.; Haase, W. *J. Am. Chem. Soc.* **1989**, *111*, 8622−8631.
(17) Watton, S. P.; Masschelein, A.; Rebek, J., Jr.; Lippard, S. J. *J. Am. Chem. Soc.* **1994**, *116*, 5196−5205.
(18) Chardon-Noblat, S.; Horner, O.; Chabut, B.; Avenier, F.; Debaeker, N.; Jones, P.; Pecaut, J.; Dubois, L.; Jeandey, C.; Oddou, J.-L.; Deronzier, A.; Latour, J.-M. *Inorg. Chem.* **2004**, *43*, 1638−1648.
(19) Kryatov, S. V.; Rybak-Akimova, E. V. *J. Chem. Soc., Dalton Trans.* **1999**, 3335−3336.
(20) Kryatov, S. V.; Nazarenko, A. Y.; Robinson, P. D.; Rybak-Akimova, E. V. *Chem. Commun.* **2000**, 921−922.
(21) Kryatov, S. V.; Chavez, F. A.; Reynolds, A. M.; Rybak-Akimova, E. V.; Que, L., Jr.; Tolman, W. B. *Inorg. Chem.* **2004**, *43*, 2141−2150.
(22) Hazell, R.; Jensen, K. B.; McKenzie, C. J.; Toflund, H. *J. Chem. Soc., Dalton Trans.* **1995**, 707−717.
(23) Poussereau, S.; Blondin, G.; Cesario, M.; Guilhem, J.; Chottard, G.; Gonnet, F.; Girerd, J.-J. *Inorg. Chem.* **1998**, *37*, 3127−3132.
(24) Zheng, H.; Zang, Y.; Dong, Y.; Young, V. G., Jr.; Que, L., Jr. *J. Am. Chem. Soc.* **1999**, *121*, 2226−2235.
(25) Kryatov, S. V.; Rybak-Akimova, E. V.; Meyer, F.; Pritzkow, H. *Eur. J. Inorg. Chem.* **2003**, 1581−1590.
(26) Lee, R. H.; Griswold, E.; Kleinberg, J. *Inorg. Chem.* **1964**, *3*, 1278−1283.

Table 1. Crystallographic Data for $[Fe_2(\mu\text{-}O)(\mu\text{-}OH)(BPMEN)_2](ClO_4)_3$ (**1**), $[Fe(BPMEN)(urea)(EtO)](ClO_4)_2$ (**2**), $[Fe_2(\mu\text{-}O)(\mu\text{-ureate})(BPMEN)_2](ClO_4)_3$ (**3**) and $[Fe_2(\mu\text{-}O)(\mu\text{-1-methylureate})(BPMEN)_2](ClO_4)_3$ (**4**)

	1	**2**	**3**·H_2O	**4**·CH_3CN
empirical formula	$C_{32}H_{45}Cl_3Fe_2N_8O_{14}$	$C_{19}H_{31}Cl_2FeN_6O_{10}$	$C_{33}H_{49}Cl_3Fe_2N_{10}O_{15}$	$C_{36}H_{52}Cl_3Fe_2N_{11}O_{14}$
formula weight (amu)	983.81	630.25	1043.87	1080.94
crystal habit, color	block, red	needle, orange	needle, green	needle, green
crystal system	monoclinic	monoclinic	orthorhombic	monoclinic
space group	*P*2(1)/*c*	*P*2(1)/*n*	*P*2(1)2(1)2(1)	*P*2(1)/*n*
a (Å)	21.4327(12)	10.145(4)	12.9520(11)	11.2585(14)
b (Å)	25.3791(14)	24.028(10)	16.2382(15)	35.284(4)
c (Å)	15.8574(8)	10.798(4)	20.5194(19)	11.9514(15)
β (deg)	110.4760(10)	98.049(8)	90	91.191(2)
V (Å^3)	8080.5(8)	2606.2(18)	4315.6(7)	4746.6(10)
Z	8	4	4	4
D_c (g cm^{-3})	1.617	1.606	1.607	1.513
crystal size (mm)	0.15 × 0.15 ×0.10	0.45 × 0.22 × 0.20	0.20 × 0.13 × 0.03	0.45 × 0.11 × 0.04
R	0.0722	0.0489	0.0878	0.0838
R_w	0.1851	0.1397	0.2000	0.2065

$[Fe(BPMEN)(urea)(EtO)](ClO_4)_2$ (2). BPMEN (109 mg, 0.40 mmol) was dissolved in 3 mL of acetonitrile/ethanol (2:1 v/v) and added to a solution of $Fe(ClO_4)_3$·$6H_2O$ (204 mg, 0.40 mmol) dissolved in 3 mL of acetonitrile/ethanol (2:1 v/v). Solid urea (24 mg, 0.40 mmol) was added to the previous mixture and the solution was stirred for 20 min. Sodium hydroxide (19 mg, 0.47 mmol) was dissolved in 2 mL of ethanol and added to the previous mixture. The resulting orange solution was left in the freezer. Orange crystals suitable for X-ray diffraction analysis were obtained overnight. Yield: 99 mg (39%). UV−vis (200−1000 nm, CH_3CN): λ_{max}, nm (ϵ, L mol^{-1} cm^{-1}) 211 (8285), 249 (10552), 340 (2819). UV−vis (200−1000 nm, solid in Nujol mull): λ_{max}, nm: 215, 251, 343. Anal. Calcd (found) for $C_{19}H_{31}N_6FeCl_2O_{10}$: C, 36.21 (36.36); H, 4.96 (4.70); N, 13.33 (12.94); Fe, 8.86 (9.41).

$[Fe_2(\mu\text{-}O)(\mu\text{-}OC(NH_2)NH)(BPMEN)_2](ClO_4)_3$ (3). Solid urea (12 mg, 0.20 mmol) was dissolved in 2.8 mL of dry acetonitrile under an argon atmosphere and added to solid complex **1a** (200 mg, 0.20 mmol). The mixture was stirred for several minutes, and then the solvent was allowed to slowly evaporate. Green crystals suitable for X-ray diffraction analysis were obtained after 2 weeks. Yield: 195 mg (95%). ^{1}H NMR (300 MHz, CD_3CN): δ (ppm) 33.6 (br), 31.8 (br), 22.2 (br), 19.5 (br), 17.33, 16.91, 15.34, 13.35 (br), 7.73 (d, J = 5 Hz), 6.57 (d, J = 5 Hz), 4.73 (br), 2.22 (s). UV−vis (400−800 nm, CH_3CN): λ_{max}, nm (ϵ, L mol^{-1} cm^{-1}): 437-(sh) (1306), 460(sh) (1145), 509 (742), 541(sh) (212), 677 (123). UV−vis (400−800 nm, solid in Nujol mull): λ_{max}, nm: 437(sh), 460(sh), 509, 541(sh), 670. ES-MS(+) (CH_3CN): *m*/*z* 925.2 ({$[Fe_2$-$(O)(OC(NH_2)NH)(BPMEN)_2](ClO_4)_2\}^+$, 100). MS-MS(+): *m*/*z* 655.0 ({$Fe_2(O)(OC(NH_2)NH)(BPMEN)(ClO_4)_2\}^+$, 100). Anal. Calcd (found) for **3**·H_2O, $C_{33}H_{49}N_{10}Fe_2Cl_3O_{15}$: C, 37.97 (38.10); H, 4.73 (4.67); N, 13.42 (13.84); Fe, 10.70 (10.94).

Complex **3** can also be directly prepared from $Fe(ClO_4)_3$·$6H_2O$ by an alternative procedure. BPMEN (27 mg, 0.10 mmol) and sodium hydroxide (4.0 mg, 0.10 mmol) were dissolved in 2 mL of acetonitrile/water (2:1 v/v). $Fe(ClO_4)_3$·$6H_2O$ (51 mg, 0.10 mmol) and urea (6.0 mg, 0.10 mmol) were dissolved in 2 mL of acetonitrile. The BPMEN/NaOH solution was added to the iron-containing solution and the mixture was left to react overnight. Vapor diffusion of diethyl ether into this solution yielded a brown precipitate after few days. Yield: 44 mg (84%). The UV−vis spectrum is identical to the spectrum of **3** prepared from **1a** and urea.

$[Fe_2(\mu\text{-}O)(\mu\text{-}OC(NHMe)NH)(BPMEN)_2](ClO_4)_3$ (4). 1-Methylurea dissolved in acetonitrile (2.5 mL, 0.05 mmol, 0.02 mol L^{-1}) was added to solid complex **1a** (50 mg, 0.05 mmol). The mixture was stirred for 4 h and then set up for vapor diffusion of diethyl ether. Green crystals suitable for X-ray diffraction analysis were obtained overnight. Yield: 48 mg (91%). For further analysis, the crystals were washed with diethyl ether, dissolved in a minimum volume of acetonitrile, and set up for a second crystallization by vapor diffusion of diethyl ether. UV−vis (400−800 nm, CH_3CN): λ_{max}, nm (ϵ, L mol^{-1} cm^{-1}): 421 (sh) (2831), 458 (sh) (2136), 510 (1028), 542(sh) (288), 678 (172). ES-MS(+) (CH_3CN): *m*/*z* 938.9 ({$[Fe_2(O)(CO(NHCH_3)NH)(BPMEN)_2](ClO_4)_2\}^+$, 3), 420.2 ({$[Fe_2$-$(O)(CO(NHCH_3)NH)(BPMEN)_2](ClO_4)\}^{2+}$, 22), 247.2 ({$[Fe_2(O)$-$(CO(NHCH_3)NH)(BPMEN)_2]\}^{3+}$, 100). Anal. Calcd (found) for $C_{34}H_{49}N_{10}Fe_2Cl_3O_{14}$: C, 39.27 (39.24); H, 4.75 (4.97); N, 13.47 (12.84); Fe, 10.74 (10.96).

X-ray Diffraction Studies. Suitable crystals of **1**−**4** were mounted on glass fibers using paratone oil. Data were collected using a Bruker SMART CCD (charge coupled device) based diffractometer equipped with an LT-3 low-temperature apparatus operating at 173 K. Data were measured using omega scans of 0.3° per frame for 30 s, such that a hemisphere was collected. A total of 1650 frames were collected with a maximum resolution of 0.75 Å. Cell parameters were retrieved using SMART[27] software and refined using SAINT on all observed reflections. Data reduction was performed using the SAINT[28] software, which corrects for Lorentzian polarization. Absorption corrections were applied on all data, except for complex **1**, using SADABS.[29] The structures were solved by the direct method using the SHELXS-97[30] program and refined by least-squares method on F^2, SHELXL-97,[31] incorporated in SHELXTL V5.10.[32] Pertinent crystallographic data and experimental conditions are summarized in Table 1. All non-hydrogen atoms were refined anisotropically. Hydrogen atoms were calculated by geometrical methods and refined as a riding model. For complex **3**, the crystal was found to be twinned and the Flack parameter was refined using the standard racemic twin law −1 0 0 0 −1 0 0 0 −1 to a value of 0.28(4). One disordered perchlorate anion was found in each of structures **1**, **3**, and **4**. Additionally, the

(27) SMART V 5.054 (NT), Software for the CCD Detector System; Bruker Analytical X-ray Systems, Madison, WI, 1998.
(28) SAINT V 6.01 (NT), Software for the CCD Detector System; Bruker Analytical X-ray Systems, Madison, WI, 1999.
(29) SADABS, Program for absorption corrections using Siemens CCD based on the method of Robert Blessing. Blessing, R. H. *Acta Crystallogr. A* **1995**, *A51*, 33−38.
(30) Sheldrick, G. M. SHELXS-90, Program for the Solution of Crystal Structure; University of Gottingen, Germany, 1990.
(31) Sheldrick, G. M. SHELXL-97, Program for the Refinement of Crystal Structure; University of Göttingen, Göttingen, Germany, 1997.
(32) SHELXTL 5.10 (PC/NT Version), Program Library for Structure Solution and Molecular Graphics; Bruker Analytical X-ray Systems, Madison, WI, 1998.

solvent molecule in structure **4** was found to occupy two different positions of 0.61 and 0.39 occupancy.

The positions of coordinated nitrogen and oxygen atoms in **3** were assigned after comparing the C(33)−O and C(33)−NH bond distances obtained for the two possible solutions. Labeling the oxygen atom as O(2), and the nitrogen atom as N(9) resulted in reasonable metric parameters. The other assignment [i.e. if O(2) is changed to NH and vice versa, N(9)H is changed to O] leads, after refinement, to a much longer bond distance for C(33)−O (d = 1.299 Å) than for C−NH (d = 1.278 Å), which is not chemically acceptable. The ureate molecule was not modeled as disordered between these two positions.

Stopped-Flow Kinetic Experiments. Rapid reactions (complete within 10^{-2}−10^{3} s) were studied using a Hi-Tech Scientific (Salisbury, Wiltshire, UK) SF-43 cryogenic stopped-flow instrument with UV−vis spectrophotometric registration and a 1.00 cm mixing cell. The kinetic data from stopped-flow experiments were treated with the integral method, using the IS-2 Rapid Kinetics software by Hi-Tech Scientific. Reactions between **1** and water, urea, or urea derivatives were studied in anhydrous acetonitrile at temperatures ranging from 5 to 50 °C. In a typical experiment, stock solutions of **1** and urea or urea derivatives were prepared under argon atmosphere at room temperature in anhydrous acetonitrile. The stock solution of urea or urea derivative was diluted to the desired concentrations (14−70 mM for urea, 28−70 mM for 1-methylurea, 7−21 mM for 1,1-dimethylurea, 56−140 mM for 1,3-dimethylurea). Water solutions (50−400 mM) were prepared individually under air atmosphere at room temperature, starting with anhydrous acetonitrile. In all cases, the concentration of **1** after mixing was 0.50 mM. All kinetic measurements were performed by monitoring the disappearance of the 555 nm absorbance band characteristic of **1**. The kinetic curves at λ = 555 nm, obtained under pseudo-first-order conditions (complex **1** as limiting reagent), were fit to equation 1:

$$A_t = A_\infty - (A_\infty - A_0)\exp(-k_{obs}t) \quad (1)$$

In all kinetic experiments, three or four shots gave standard deviations for k_{obs} below 4%.

Regular UV−Vis Kinetic Experiments. Reactions with longer time scale (10^{4}−10^{5} s) were studied using a Hitachi U-2000 spectrophotometer or a JASCO V-570 spectrophotometer. The second step of the reactions between **1** and urea, 1-methylurea, 1,1-dimethylurea, and acetamide were studied in anhydrous acetonitrile at 25 °C. Solutions of urea and 1,1-dimethylurea were prepared under argon atmosphere and added to solid iron complex **1a** previously weighed and dried in a cell. In the case of 1-methylurea and acetamide, a concentrated solution was added to a solution of **1**. In all cases, the mixing time before starting the acquisition was 30 s and the concentration of **1** after mixing was 1.0 mM. The kinetic traces were obtained by taking full spectra (from 400 to 800 nm) at defined time intervals and looking at the cross section at 555 nm or by directly monitoring the absorbance at 555 nm versus time for several hours. Kinetic data were treated similarly to those obtained by stopped-flow methods.

ESI Mass Spectrometry. In situ electrospray mass spectra were obtained using a Finnigan LTQ mass spectrometer. The analysis was performed at room temperature for the reactions of **1** with urea, 1-methylurea, 1,1-dimethylurea, and 1,3-dimethylurea. In a typical experiment, stock solutions of **1** and urea were prepared in anhydrous air-free acetonitrile and mixed in a 1:50 molar ratio. Samples were 0.33 mM in **1**. Analysis of the reaction mixtures was performed at reaction times of 10 min and 14 h.

Urea Hydrolysis Studies. Ammonia production was assayed using the indophenol assay procedure described by Barrios et al.[33] The incubation time prior to UV−vis analysis was one night in order to let the iron residues precipitate out. In a typical experiment, a solution of **1** was mixed with equimolar amounts or excess of urea (up to 7 equiv) in the presence or in the absence of water (up to 100 equiv). The concentration of **1** after mixing was 10 mM and blank samples without **1** were also prepared. Aliquots (50 μL) were analyzed after 1 h and after 1 day of reaction at 4, 23, and 60 °C. A similar procedure was followed for urea hydrolysis studies with complex **3**.

Results

Synthesis of Complexes. Complex [Fe_2(μ-O)(μ-OH)-(BPMEN)$_2$](ClO_4)$_3$ (**1**) featuring a rare (μ-oxo)(μ-hydroxo)-diiron(III) core has been identified spectroscopically from the dissolution of the hydrated form [Fe_2(μ-O)(OH)(OH_2)-(BPMEN)$_2$](ClO_4)$_3$ (**1a**) in dry acetonitrile.[23,24] The hydrated form (**1a**) was well-characterized as a solid, including an X-ray crystal structure determination.[23] In our hands, the reported synthetic procedure[23] used to obtain **1a** yielded, in different batches, either green crystals of pure **1a** or a maroon powder, which is mainly composed of dark-red **1** with a small amount of **1a** (see ESI). A similar published procedure reported maroon crystals formulated as **1**·2H_2O without structural characterization.[22] In all reports[22−24] and in our hands, the UV−vis spectra of either green or maroon solids in dry acetonitrile were identical, indicating that dark-red complex **1** is the dominant species in such solutions. We obtained analytically pure solid complex **1** in good yield by the recrystallization of **1a** from anhydrous acetonitrile under argon atmosphere (Scheme 2). The solid-state UV−vis spectrum of complex **1** presents a characteristic intense feature at 555 nm previously observed in solution,[23,24] confirming the assignment of solid **1** as [Fe_2(μ-O)(μ-OH)-(BPMEN)$_2$](ClO_4)$_3$.

Complex **1** reacts in acetonitrile solution with urea, yielding eventually yellow complex [Fe_2(μ-O)(μ-OC(NH_2)-NH)(BPMEN)$_2$](ClO_4)$_3$ (**3**) (Scheme 2). An analogous procedure with 1-methylurea gives complex [Fe_2(μ-O)(μ-OC(NHMe)NH)(BPMEN)$_2$](ClO_4)$_3$ (**4**). Complex **3** can be also obtained by self-assembly of Fe(ClO_4)$_3$, BPMEN, and urea under the action of sodium hydroxide in acetonitrile/water. An attempt at the self-assembly synthesis in acetonitrile/ethanol afforded complex [Fe(BPMEN)(urea)(EtO)]-(ClO_4)$_2$ (**2**) (Scheme 2). The synthetic procedures for complexes **1**−**4** were repeated several times, proving their reproducibility.

The solid-state FTIR spectrum of complex **3** exhibits several features due to the presence of urea ligand, which are absent in complex **1**: a carbonyl stretching frequency at 1656 cm^{-1} and the NH_2 group vibrations between 3330 and 3180 cm^{-1}. Similarly, the solid-state FTIR spectrum of complex **2** exhibits a carbonyl stretching frequency at 1666 cm^{-1} and features between 3340 and 3200 cm^{-1}. These

(33) Barrios, A. M.; Lippard, S. J. *J. Am. Chem. Soc.* **1999**, *121*, 11751−11757.

Scheme 2. Synthetic Routes to Complexes **1**−**4**

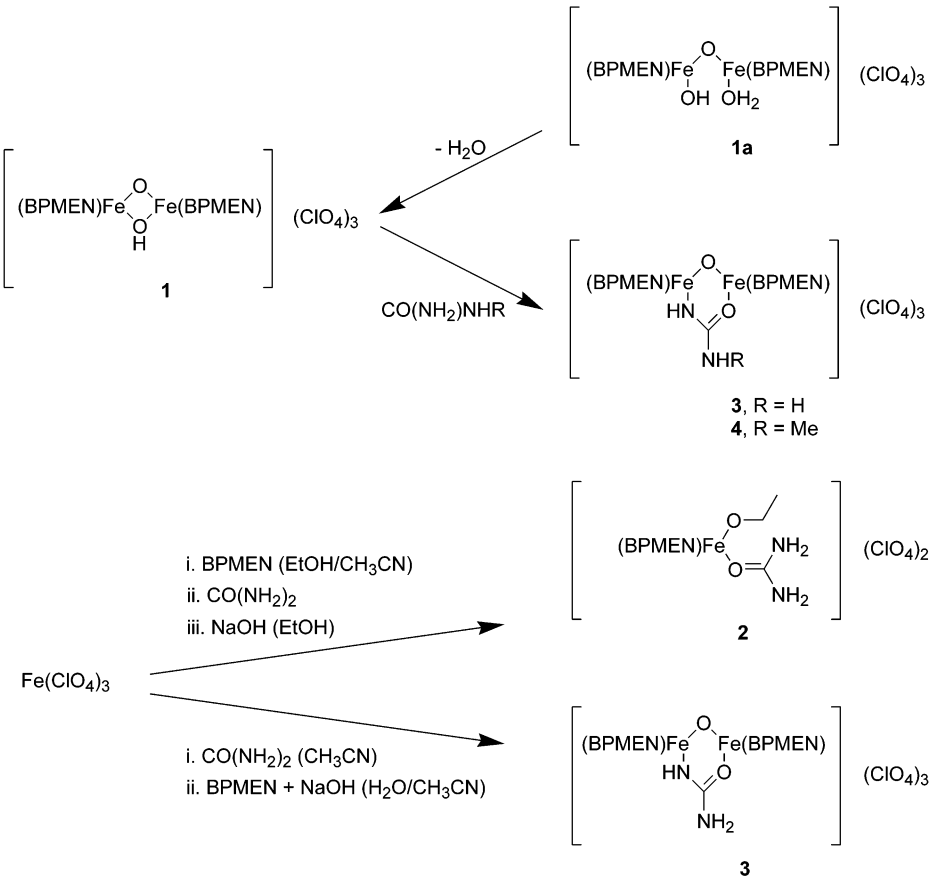

values are in agreement with literature reports on metal−urea complexes.[34]

Structure of Complex 1. As determined by the X-ray diffraction analysis, complex $[Fe_2(\mu\text{-O})(\mu\text{-OH})(BPMEN)_2](ClO_4)_3$ (**1**) contains the (μ-oxo)(μ-hydroxo)diiron(III) core with BPMEN acting as a tetradentate N_4 ligand and completing the distorted octahedral environment of each iron atom (Figure 1, Table 2). Like in all previously characterized

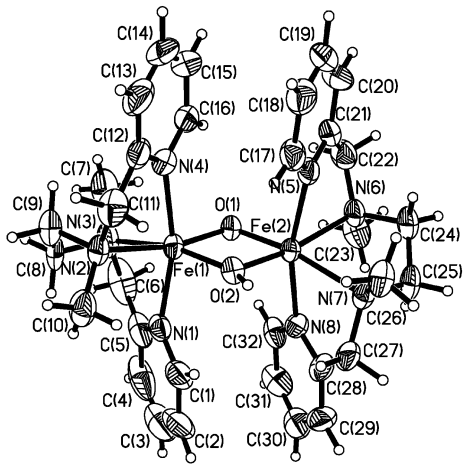

Figure 1. Representation of the X-ray structure of the complex cation in **1** (molecule A), showing 50% probability thermal ellipsoids.

Table 2. Selected Bond Lengths (Å) and Bond Angles (deg) for $[Fe_2(\mu\text{-O})(\mu\text{-OH})(BPMEN)_2](ClO_4)_3$ (**1**)

	molecule A		molecule B	
	Fe1	Fe2	Fe3	Fe4
Fe−O	1.884(4) (O1)	1.892(4) (O1)	1.856(4) (O3)	1.862(4) (O3)
Fe−OH	1.906(4) (O2)	1.912(4) (O2)	1.965(4) (O4)	1.955(4) (O4)
Fe−N	2.215(5) (N2)	2.181(5) (N6)	2.179(5) (N10)	2.198(5) (N14)
(in-plane)	2.226(5) (N3)	2.222(5) (N7)	2.227(5) (N11)	2.246(5) (N15)
Fe−N	2.115(5) (N1)	2.150(5) (N8)	2.145(5) (N12)	2.125(6) (N16)
(out-of-plane)	2.124(5) (N4)	2.156(5) (N5)	2.166(5) (N9)	2.145(5) (N13)
Fe···Fe	2.8212(11)		2.8267(11)	
Fe−O−Fe	96.68(19)		98.98(18)	
Fe−OH−Fe	95.28(18)		92.32(18)	

diiron(III) complexes of BPMEN,[22,23,35−37] this ligand adopts a cis-α conformation with the pyridine groups in the axial positions. The solid-state structure of **1** reveals two crystallographically unique but chemically identical complex cations (A and B) per asymmetric unit. In both cations, the hydroxide proton is hydrogen bonded to a perchlorate ion. The distinction between the oxo bridge and the hydroxo bridge is also pronounced in the bond lengths: the average Fe−(μ-O) bond (1.87 Å) is shorter than the average Fe−(μ-OH) bond (1.93 Å). The average Fe−O−Fe angle is 97.8°, and the average Fe−OH−Fe angle is 93.8°. These results are consistent with previous findings concerning the $Fe_2(\mu$-O)-

(34) Theophanides, T.; Harvey, P. D. *Coord. Chem. Rev.* **1987**, *76*, 237−264.

(35) Egdal, R. K.; Hazell, R.; McKenzie, C. J. *Acta Crystallogr. C* **2002**, *E58*, m10-m12.

(36) Okuno, T.; Ito, S.; Ohba, S.; Nishida, Y. *J. Chem. Soc., Dalton Trans.* **1997**, 3547−3551.

(37) Arulsamy, N.; Goodson, P. A.; Hodgson, D. J. *Inorg. Chim. Acta* **1994**, *216*, 21−29.

Table 3. Selected Bond Lengths (Å) and Bond Angles (deg) for [Fe(BPMEN)(urea)(EtO)](ClO$_4$)$_2$ (**2**), [Fe$_2$(μ-O)(μ-ureate)(BPMEN)$_2$](ClO$_4$)$_3$ (**3**), and [Fe$_2$(μ-O)(μ-1-methylureate)(BPMEN)$_2$](ClO$_4$)$_3$ (**4**)[a]

	2	**3**·H$_2$O	**4**·CH$_3$CN
C−O(urea)	1.275(3)	1.287(9)	1.293(7)
C−NH(urea)	−	1.290(9)	1.319(8)
C−NHX (urea)	1.329(3)	1.365(11)	1.341(8)
	1.318(3)		
Fe−O(urea)	1.9932(18)	1.985(6)	1.967(4)
Fe−N(urea)	−	1.968(6)	1.994(5)
Fe−O(Et)	1.824(2)	−	−
Fe−N(L)	2.196(2) (N2)	2.345(7) (N2)	2.204(5) (N2)
in-plane	2.237(2) (N3)	2.198(8) (N3)	2.284(5) (N3)
		2.300(6) (N6)	2.231(5) (N6)
		2.202(7) (N7)	2.304(5) (N7)
Fe−N(L)	2.131(2) (N1)	2.178(8) (N4)	2.144(5) (N4)
out-of-plane	2.138(2) (N4)	2.132(9) (N1)	2.153(5) (N1)
		2.145(9) (N5)	2.158(5) (N5)
		2.176(9) (N8)	2.167(5) (N8)
Fe−O−Fe	−	130.8(3)	129.1(2)
Fe−O−C(Et)	142.42(17)	−	−

[a] X = H, CH$_3$; L = BPMEN.

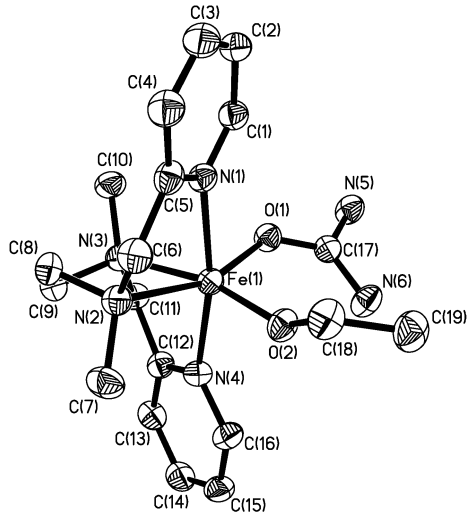

Figure 2. Representation of the X-ray structure of the complex cation in **2**, showing 50% probability thermal ellipsoids. Hydrogen atoms are not included for clarity.

(μ-OH) cores.[15,24,38,39] The Fe(μ-O)(μ-OH)Fe core in complex **1** is more symmetric than the oxo−hydroxo diiron(III) core in the analogous but more sterically constrained complex with the related ligand BPMCN (derived from cyclohexenediamine in place of ethylenediamine).[39]

The value for the Fe−O−Fe angle in complex **1** determined from crystallographic data is smaller than expected from electronic spectra measurements: an angle of 111° was predicted from the UV−vis spectrum of **1** in acetonitrile by Poussereau et al.[23] However, that calculation was based on the extrapolation of a linear correlation between the Fe−O−Fe angle and the near-IR band observed in the 500−550 nm region for angles ranging from 125° to 138°.[23,40] Resonance Raman spectroscopy was used more successfully to predict the Fe−O−Fe angle in complex **1**.[22−24] This analysis was based on the correlation between vibrational frequencies for the Fe−O−Fe symmetric stretches with the observed angle as described by Sanders-Loehr et al.[41] An intense band at 593 cm^{-1} (according to Hazell et al.[22]) or at 600 cm^{-1} (according to Poussereau et al.[23]) was reported for complex **1**, predicting an angle of 100° or 98°, respectively. These values are very close to the angle obtained by X-ray analysis in this work.

Structures of Complexes 2−4 Containing Urea Ligands. The molecular structures of **2**−**4** were determined, and their metric parameters are compared in Table 3.

The structure of the complex cation of [Fe(BPMEN)(urea)(EtO)](ClO$_4$)$_2$ (**2**) (Figure 2) shows a six-coordinate iron(III) center with four coordination sites occupied by the nitrogen atoms of the BPMEN ligand, one site occupied by an ethoxy ligand, and the last site occupied by an O-bound neutral urea ligand.

Complex **2** is the second prepared and characterized mononuclear iron(III) complex of the BPMEN ligand. The cis-α conformation of BPMEN is similar to the previously characterized diiron(III) complexes of this ligand[20,22,23,35−37] and to the mononuclear iron(III) complex [Fe(BPMEN)(DBC)](BPh$_4$)[42] and iron(II) complex [Fe(BPMEN)(CH$_3$CN)$_2$](ClO$_4$)$_2$.[43,44] The Fe−N bond lengths (2.13−2.24 Å) for **2** are in the typical range for high-spin iron(III) complexes. The presence of a terminal ethoxy ligand in the structure is confirmed by a short iron−oxygen (Fe1−O2) bond distance of 1.82 Å [EtOH would lead to a weaker binding with *d*(Fe−O) of about 2.15 Å].[45−48] Very few other examples of mononuclear iron(III) alkoxide complexes have been structurally characterized and reported in the literature. Most of the known structures were obtained for heme iron(III) complexes with a methoxy group bound to the metal center in the axial position[49−55] and, to our knowledge, only

(38) Furutachi, H.; Ohyama, Y.; Tsuchiya, Y.; Hashimoto, K.; Fujinami, S.; Uehara, A.; Suzuki, M.; Maeda, Y. *Chem. Lett.* **2000**, 1132−1133.
(39) Stubna, A.; Jo, D.-H.; Costas, M.; Brenessel, W. W.; Andres, H.; Bominaar, E. L.; Münk, E.; Que, L., Jr. *Inorg. Chem.* **2004**, *43*, 3067−3079.
(40) Norman, R. E.; Holz, R. C.; Ménage, S.; O'Connor, C. J.; Zhang, J. H.; Que, L., Jr. *Inorg. Chem.* **1990**, *29*, 4629−4637.
(41) Sanders-Loehr, J.; Wheeler, W. D.; Shiemke, A. K.; Averill, B. A.; Loehr, T. M. *J. Am. Chem. Soc.* **1989**, *111*, 8084−8093.
(42) Mialane, P.; Tchertanov, L.; Banse, F.; Sainton, J.; Girerd, J.-J. *Inorg. Chem.* **2000**, *39*, 2440−2444.
(43) Chen, K.; Que, L., Jr. *Chem. Commun.* **1999**, 1375−1376.
(44) Quinonero, D.; Musaev, D. G.; Morokuma, K. *Inorg. Chem.* **2003**, *42*, 8449−8455.
(45) Kajiwara, T.; Tasuku, I. *Acta Crystallogr. C* **2000**, *C56*, 22−23.
(46) Scheidt, W. R.; Geiger, D. K.; Lee, Y. J.; Gans, P.; Marchon, J.-C. *Inorg. Chem.* **1992**, *31*, 2660.
(47) Gans, P.; Buisson, G.; Duee, E.; Regnard, J.-R.; Marchon, J.-C. *Chem. Commun.* **1979**, 393.
(48) Bertrand, J. A.; Fujita, E.; Eller, P. G.; VanDerveer, D. G. *Inorg. Chem.* **1978**, *17*, 3571.
(49) Johnson, M. R.; Seok, W. K.; Ma, W.; Slebodnick, C.; Wilkoxen, K. M.; Ibers, J. A. *J. Org. Chem.* **1996**, *61*, 3298−3303.
(50) Prevot, L.; Jaquinot, L.; Fisher, J.; Weiss, R. *Inorg. Chim. Acta* **1998**, *283*, 98−104.
(51) Hoard, J. L.; Hamor, M. J.; Hamor, T. A.; Caughey, W. S. *J. Am. Chem. Soc.* **1965**, *87*, 2312−2319.
(52) Potz, R.; Huckstadt, H.; Homborg, H. Z. *Z. Anorg. Allg. Chem.* **1998**, *624*, 173.
(53) Kim, Y.; Nam, W.; Lim, S.-J.; Lough, A. J.; Kim, S.-J. *Acta Crystallogr. C* **2001**, *57*, 556.
(54) Hatano, K.; Uno, T. *Bull. Chem. Soc. Jpn.* **1990**, *63*, 1825.
(55) Lecomte, C.; Chadwick, D. L.; Coppens, P.; Stevens, E. D. *Inorg. Chem.* **1983**, *22*, 2982.

four structures for mononuclear non-heme iron(III) alkoxide complexes[56−58] have been reported. The iron−oxygen bond distance in complex **2** is elongated as compared to the other non-heme iron complexes (1.77−1.80 Å)[56−58] but shorter than most Fe−OR distances found in heme complexes (about 1.84 Å).[49−55] The Fe−O−C angle (142°) is consistent with the absence of multiple Fe−OEt bonding, which would lead to a linear arrangement of Fe−O−R.[56−58] Complex **2** is also one of the few structurally characterized iron complexes with a neutral urea ligand, with previous determinations limited to $[Fe(urea)_6]^{3+}$ [59] and $[Fe(urea)_6]^{2+}$.[60] Like in most transition metal complexes containing this ligand, urea in complex **2** binds through its oxygen.[34] Metric parameters of the O-bonded urea ligand in **2** [d(C−O) = 1.28 Å and average d(C−N) = 1.32 Å] also agree well with those found in other metal complexes. The carbonyl bond in metal-bonded urea is longer and the C−N bond shorter compared to free urea in a vacuum determined by microwave spectroscopy [d(C−O) = 1.22 Å and d(C−N) = 1.38 Å].[61] It is interesting to note that the metric parameters of the urea molecule in crystals of pure urea [d(C−O) = 1.26 Å and d(C−N) = 1.35 Å][62] are intermediate between those in metal complexes and those in a vacuum, apparently reflecting the influence of the strong hydrogen bonds in solid urea comparable in effect with the coordination to a metal ion. The iron−oxygen distance (1.99 Å) in **2** is similar to that observed in the iron(III) complex $[Fe(urea)_6]^{3+}$ [d(Fe−O) = 2.03 Å].[59]

Complexes **3** and **4** are structurally similar to each other and consist of two Fe^{III}(BPMEN) moieties bridged by an oxo ligand and an N,O-coordinated ureate anion ligand (Figure 3). These structures confirm that **3** and **4** are derived from complex **1** by substituting a hydroxy ligand for an ureate ligand. Upon substitution, the four-membered Fe^{III}-(μ-O)(μ-OH)Fe^{III} core is converted to a nearly flat six-membered Fe^{III}(μ-O)(μ-OC(NHR)NH)Fe^{III} core (R = H, Me), and the Fe−O−Fe angle expands from 97.8° (**1**) to 130.8° (**3**) or 129.1° (**4**) (Table 3). The structures of complexes **3** and **4** are close to related compounds $[Fe_2(O)(\mu\text{-}OC(NH_2)NH)(TPA)_2](ClO_4)_3$ [20] and $[Fe_2(O)(\mu\text{-}O_2CCH_3)(BPMEN)_2](ClO_4)_3$ (**5**).[36] The structural similarities between the ureate complex **3** and the acetate complex **5** confirm that complex **3** contains deprotonated urea ligand H_2NCONH^- isoelectronic to $CH_3CO_2^-$. The coordination mode of BPMEN in **3** and **4** is similar to other Fe(III) complexes of this ligand,[22,23,35−37] including **1** and **2** discussed above.

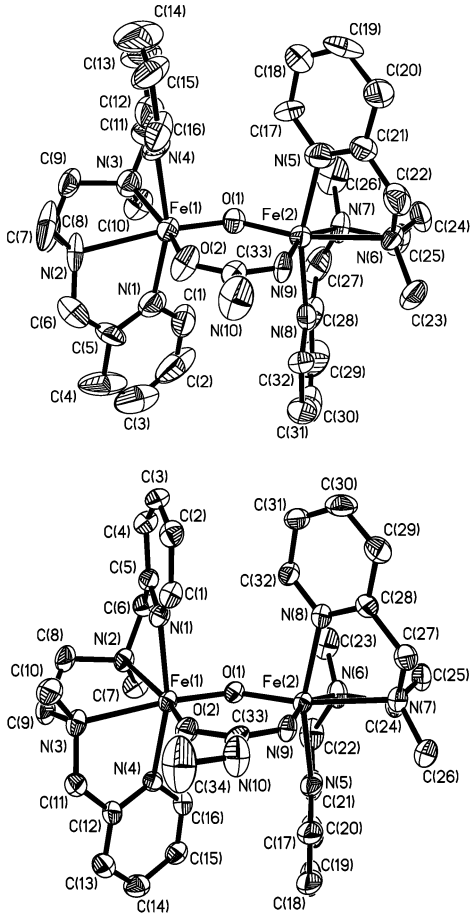

Figure 3. Representation of the X-ray structure of the complex cations in **3** (top) and **4** (bottom), showing 50% probability thermal ellipsoids. Hydrogen atoms are not included for clarity.

Mechanistic Studies of the Reactions between $[Fe_2(\mu\text{-}O)(\mu\text{-}OH)(BPMEN)_2]^{3+}$ (1) and Urea or Structural Analogues of Urea. The reactivity of complex **1** with urea and its structural analogues was investigated in acetonitrile solutions (Scheme 3). Unlike the analogous diiron(III) complex $[Fe_2(\mu\text{-}O)(OH)(OH_2)(TPA)_2]^{3+}$, which slowly reacted with acetonitrile to produce the acetamide complex $[Fe_2(\mu\text{-}O)(\mu\text{-}OC(CH_3)NH)(TPA)_2]^{3+}$,[63] complex **1** is stable in acetonitrile solution at room temperature for days, as seen from the unchanged characteristic UV−vis spectrum of **1** featuring intense absorption at 555 nm (ϵ = 890 M^{-1} cm^{-1}). Therefore, acetonitrile is suitable as a solvent to study the reactivity of **1** with other ligands.

Urea, 1-methylurea, 1,1-dimethylurea, and acetamide react with **1** in two distinct steps (Scheme 3). The first, rapid step of the reaction is accompanied by a characteristic drop in absorbance at all wavelengths in the UV−vis spectrum, indicative of the formation of a ring-opened intermediate. The composition of the intermediate was confirmed by in situ mass spectrometry. The second, slow reaction step, which yields the ring-closed products with bridging ureates or acetamidate, involves elimination of a water molecule and binding of the deprotonated nitrogen. This formulation is

(56) Jonas, R. T.; Stack, T. D. P. *J. Am. Chem. Soc.* **1997**, *119*, 8566−8567.
(57) O'Keefe, B. J.; Breyfogle, L. E.; Hillmyer, M. A.; Tolman, W. B. *J. Am. Chem. Soc.* **2002**, *124*, 4384−4393.
(58) Roelfes, G.; Lubben, M.; Chen, K.; Ho, R. Y. N.; Meetsma, A.; Genseberger, S.; Hermant, R. M.; Hage, R.; Mandal, S. K.; Young, V. G., Jr.; Zang, Y.; Kooijman, H.; Spek, A. L.; Que, L., Jr.; Feringa, B. L. *Inorg. Chem.* **1999**, *38*, 1929−1936.
(59) Kuz'mina, N. E.; Palkina, K. K.; Savinkina, E. V. *Zh. Neorg. Khim. (Russ.) (Russ. J. Inorg. Chem.)* **1999**, *44*, 1988.
(60) Kuz'mina, N. E.; Palkina, K. K.; Savinkina, E. V.; Kozlova, I. A. *Zh. Neorg. Khim. (Russ.) (Russ. J. Inorg. Chem.)* **2000**, *45*, 395.
(61) Godfrey, P. D.; Brown, R. D.; Hunter, A. N. *J. Mol. Struct.* **1997**, *413*−*414*, 405−414.
(62) Scheringer, C. *Acta Crystallogr. A* **1980**, *36*, 814−818.
(63) Wilkinson, E. C.; Dong, Y.; Que, L., Jr. *J. Am. Chem. Soc.* **1994**, *116*, 8394−8395.

Scheme 3. Series of Reactions Studied in This Work and Numbering of Some of the Species Involved

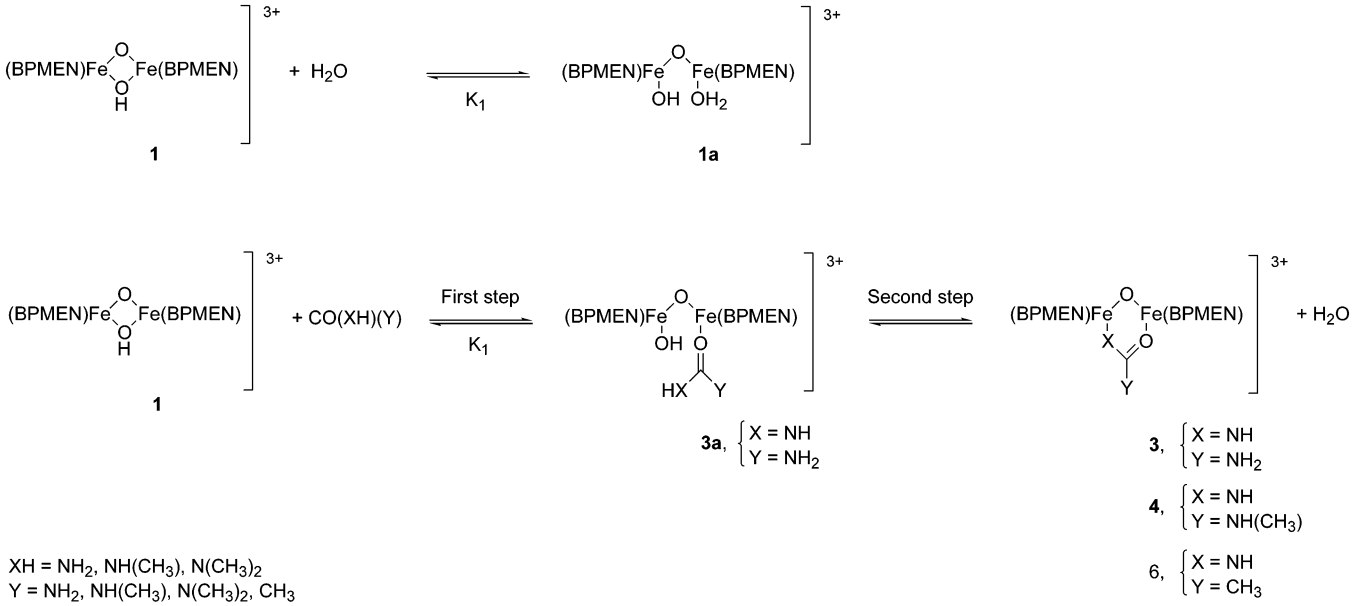

consistent with the UV−vis and mass-spectrometry data (see below). Products of the reaction with urea (**3**) and 1-methylurea (**4**) were structurally characterized (Figure 3). *N*,*N*′-substituted ureas (1,3-dimethylurea and 1,1,3,3-tetramethylurea) also reacted with complex **1**, but only via the first step shown in Scheme 3. No ring-closed products were obtained with these ligands.

Ring Opening of the (μ-Oxo)(μ-hydroxo)diiron(III) Core. Time-resolved UV−vis spectra for the first reaction step between **1** and urea derivatives show the disappearance of the 555 nm band. These spectral changes (Figure 4)

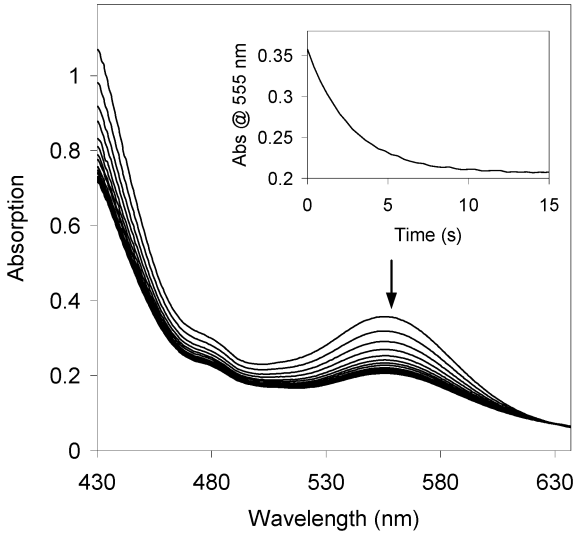

Figure 4. Time-resolved UV−vis spectra for the first step of the reaction between **1** and urea acquired in the diode array mode using stopped-flow techniques (0.50 mM of **1** and 35 mM of urea after mixing at 25 °C in acetonitrile). The insert shows the corresponding kinetic trace at 555 nm.

indicate that the four-membered Fe^{III}(μ-O)(μ-OH)Fe^{III} core has been opened or expanded. As shown by Que and co-workers, electronic spectra of (μ-oxo)diiron(III) complexes are characteristic of the Fe−O−Fe angle: acute angles of ca. 100° are associated with the intense absorbance near 550 nm, and this band loses intensity and shifts to a lower wavelength as the angle increases.[24] Such shift was also observed in the reactions of **1** with HSO_4^- or with carboxylic acids.[22]

The reactions shown in Scheme 3 were also followed by mass spectrometry. For example, the intermediate obtained by reacting **1** with 1,1-dimethylurea has been clearly detected by in situ mass spectrometry after 10 min of reaction as a 100% peak at *m*/*z* 257.6, corresponding to $\{[Fe_2(\mu\text{-O})(OH)(CO(NH_2)(N(CH_3)_2))(BPMEN)_2]\}^{3+}$ (see ESI). This peak was not present in the spectrum of the starting material **1**, and its isotopic pattern confirms the composition of this intermediate. After 14 h of reaction, the peak at *m*/*z* 257.6 is barely detectable and a new base peak appears at *m*/*z* 251.7, corresponding to the ring-closed product $\{[Fe_2(\mu\text{-O})(\mu\text{-CO}(NH)(N(CH_3)_2))(BPMEN)_2]\}^{3+}$. Smaller peaks corresponding to different ionization states of this complex were also identified at *m*/*z* 427.2 ($\{[Fe_2(\mu\text{-O})(\mu\text{-CO}(NH)(N(CH_3)_2))(BPMEN)_2](ClO_4)\}^{2+}$, 17%) and 952.9 ($\{[Fe_2(\mu\text{-O})(\mu\text{-CO}(NH)(N(CH_3)_2))(BPMEN)_2](ClO_4)_2\}^{+}$, 4%). The intermediate obtained by reacting **1** with 1-methylurea has also been clearly detected after 10 min of reaction as a 100% peak at *m*/*z* 252.9 corresponding to $\{[Fe_2(\mu\text{-O})(CO(NH_2)(NH(CH_3)))(BPMEN)_2]\}^{3+}$. Upon mixing **1** and urea, a smaller peak has been observed at *m*/*z* 248.4 corresponding to the intermediate $\{[Fe_2(\mu\text{-O})(OH)(CO(NH_2)NH_2)(BPMEN)_2]\}^{3+}$. In both cases, the spectra after 14 h resemble those of the ring-closed species **3** and **4** (see Experimental Section). Upon mixing **1** with 1,3-dimethylurea, a 100% peak at *m*/*z* 257.6 corresponding to $\{[Fe_2(\mu\text{-O})(OH)(CO(NH(CH_3))\ (NH(CH_3)))(BPMEN)_2]\}^{3+}$ was also observed. The spectra taken after 10 min and 14 h, however, were identical in this case. This indicates that the formation of a 1:1 adduct between **1** and a substituted urea occurs even for the ligands that do not undergo ring closure.

A reaction similar to adduct formation between **1** and urea derivatives is water addition to **1**. The reaction between **1**

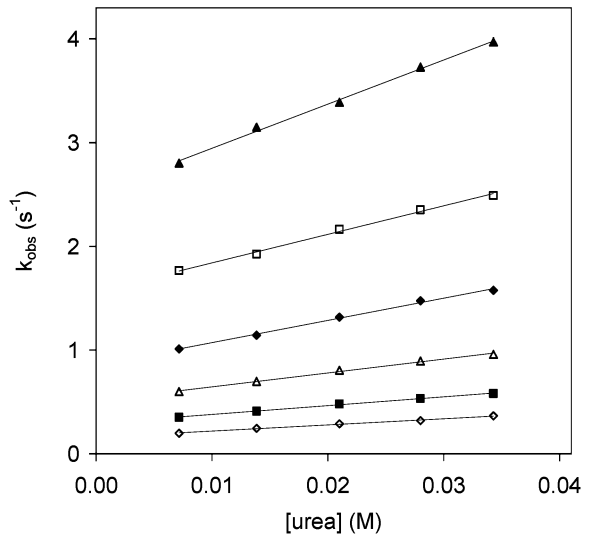

Figure 5. Plot of the observed rate constant at 555 nm versus urea concentration after mixing with **1** acquired by stopped-flow technique at different temperatures (0.50 mM of **1** and 7−35 mM of urea after mixing): $T = 25$ °C (◇), 30 °C (■), 35 °C (△), 40 °C (◆), 45 °C (□), and 50 °C (▲).

and water is reversible and leads to the formation of the already known ring-opened hydrated species $[Fe_2(\mu\text{-O})(OH)(OH_2)(BPMEN)_2](ClO_4)_3 \cdot H_2O$ (**1a**).[23] A detailed kinetic study of this process is reported here and compared to related processes depicted in Scheme 3.

The rates of (usually) rapid reactions between complex **1** and additional ligands (water or urea derivatives) were determined by stopped-flow techniques.

Extensive concentration and temperature dependency experiments were performed with water, urea, 1-methylurea, and 1,3-dimethylurea (see Experimental Section). All reactions follow a single exponential change of optical absorbance in the presence of a large excess of water, urea, or its analogues, indicating first-order in complex **1**:

$$v = k_{obs}[\mathbf{1}] \tag{2}$$

The plots of the observed rate constant versus ligand concentration under pseudo-first-order conditions are straight lines with nonzero intercepts (Figures 5, S7, S9, and S10). This kinetic behavior may result from a reversible bimolecular reaction. In this case, the rate law has two terms

$$k_{obs} = k_1[\mathrm{L}] + k_{-1} \tag{3}$$

where k_1 is the rate constant of the forward reaction (ligand binding) and k_{-1} is the rate constant for the reverse reaction (ligand dissociation)

$$\mathbf{1} + \mathrm{L} \underset{k_{-1}}{\overset{k_1}{\rightleftharpoons}} \mathbf{1}(\mathrm{L}),\ K_1 = k_1/k_{-1} \tag{4}$$

By combination of the appropriate kinetic parameters for the corresponding forward and reverse reaction ($K_1 = k_1/k_{-1}$) or by direct analysis of rapid equilibrium, thermodynamic parameters have been derived (Table 4). For example, "rapid spectrophotometric titrations" of complex **1** with urea allowed us to calculate the equilibrium constant for the monodentate urea binding at 25 °C by using the values of A_∞ and A_0 at several concentrations of urea (eq 1). The value for K_1 obtained by this method (44 ± 5 L mol^{-1}) is very close to the one determined from the rate constants for urea binding and dissociation (37 ± 2 L mol^{-1}). Similarly, spectrophotometric titrations of **1** with water gave an equilibrium constant for reversible hydration (2.9 ± 0.1 L mol^{-1}) that was close to the ratio of k_1/k_{-1} (1.8 ± 0.1 L mol^{-1}). Good agreement between direct measurements of equilibrium constants and the values of equilibrium constants derived from kinetic data support the simple model depicted in Scheme 3 and eqs 3 and 4. The values of K_1 reported in Table 4 for water, urea, 1-methylurea, 1,1-dimethylurea, and 1,3-dimethylurea were calculated from kinetic data recorded by stopped-flow techniques as described above. However, for tetramethylurea and acetamide, a regular UV−vis approach was used, since the open species were stable enough (see ESI). Kinetic and thermodynamic parameters of the ring-opening process (first step, Scheme 3) for all ligands are summarized in Tables 4, S2, and S3.

The observed rate constants at different concentrations of the ligands were also measured as a function of temperature, yielding the values of k_1 and k_{-1} for the temperature range from 5 to 50 °C (Figures 5, S7, S9, and S10, Tables S2 and S3). The activation enthalpies and entropies for ligand binding and ligand dissociation, which were calculated from linear Eyring or Arrhenius plots (Figures 6, S8, S11, and S12), are summarized in Table 4.

Ring Closure and Formation of the Ureate or Acetamidate Complexes. This reaction was observed for ligands that have at least one nonmethylated amide group $RCONH_2$ ($R = NH_2$, $NHCH_3$, $N(CH_3)_2$, CH_3). The products of the ring closure were fully characterized for the reactions of **1** with urea and 1-methylurea (complexes **3** and **4**, respectively). With 1,1-dimethylurea and acetamide, similar spectral changes were observed and attributed to the same ring-closure process. Figure 7 shows a typical time-resolved spectral change observed for the reaction between **1** and urea to form **3**.

The electronic spectra for the final products obtained in reactions of **1** with urea, 1-methylurea, 1,1-dimethylurea, and acetamide are summarized in Table 5 and compared to that of known acetate bridged $[Fe_2(\mu\text{-O})(\mu\text{-}CH_3CO_2)(BPMEN)_2](ClO_4)_3$ (**5**).[36] All complexes present the characteristic features between 400 and 550 nm in their electronic spectra indicative of doubly bridged species, with less acute angles than those in the $Fe^{III}(O)(OH)Fe^{III}$ diamond core species,[24] as previously described for **5** and other carboxylate complexes.[40,64,65] While spectra of the complexes with bridged ureate, methylated ureate, or acetate are similar and present the same general features, they display distinct differences in the 400−480 nm region. However, the spectra of the bridged acetamide complex $[Fe_2(\mu\text{-O})(\mu\text{-}OC(NH)CH_3)(BPMEN)_2](ClO_4)_3$ (**6**) and the bridged acetate complex **5** appear to be almost identical. Two lines of evidence argue

(64) Yan, S.; Cox, D. D.; Pearce, L. L.; Juarez-Garcia, C.; Que, L., Jr.; Zhang, J. H.; O'Connor, C. J. *Inorg. Chem.* **1989**, *28*, 2509−2511.
(65) Holz, R. C.; Elgren, T. E.; Pearce, L. L.; Zhang, J. H.; O'Connor, C. J.; Que, L., Jr. *Inorg. Chem.* **1993**, *32*, 5844−5850.

Table 4. Comparison of the Kinetic and Thermodynamic Parameters for Water, Urea, Methylated Ureas, and Acetamide Interaction with Complex **1** at 25 °C in Acetonitrile

incoming/leaving ligand	water	urea	1-methylurea	1,1-dimethylurea	1,3-dimethylurea	1,1,3,3-tetramethylurea	acetamide
first step k_1 (M^{-1} s^{-1})	1.6 ± 0.1	5.9 ± 0.2	3.2 ± 0.1	6.7 ± 0.5	1.5 ± 0.1	−	−
$\Delta H^{\ddagger}_1$ (kJ mol^{-1})	61 ± 2	61 ± 2	60 ± 2	−	63 ± 3	−	−
$\Delta S^{\ddagger}_1$ (J mol^{-1} K^{-1})	−43 ± 1	−25.2 ± 0.7	−31.7 ± 0.8	−	−29 ± 1	−	−
first step $k_{-1} \times 10^1$ (s^{-1})	8.6 ± 0.1	1.61 ± 0.05	0.95 ± 0.03	1.83 ± 0.04	1.48 ± 0.06	−	−
$\Delta H^{\ddagger}_{-1}$ (kJ mol^{-1})	90.5 ± 0.8	86 ± 1	90 ± 1	−	92 ± 1	−	−
$\Delta S^{\ddagger}_{-1}$ (J mol^{-1} K^{-1})	49.7 ± 0.5	28.2 ± 0.3	38.9 ± 0.4	−	48.1 ± 0.6	−	−
preequilibrium K_1 (L mol^{-1})	1.8 ± 0.1	37 ± 2	33 ± 2	37 ± 3	9.9 ± 0.8	1.2 ± 0.1[a]	19 ± 2[a]
$\Delta H°$(kJ mol^{-1})	−29 ± 2	−25 ± 2	−30 ± 2	−	−29 ± 3	−	−
$\Delta S°$(J mol^{-1} K^{-1})	−93 ± 1	−53.4 ± 0.8	−70.6 ± 0.9	−	−77 ± 1	−	−
second step $k_2 \times 10^4$ (s^{-1})	−	6.6 ± 0.6	1.2 ± 0.4	0.5 ± 0.2	−	−	0.11 ± 0.04

[a] Constant determined by direct analysis of rapid equilibrium using regular UV−vis techniques.

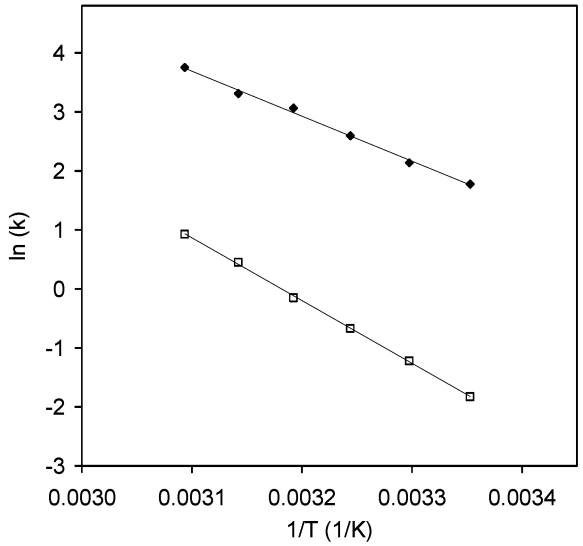

Figure 6. Arrhenius plots for the forward (◆) and reverse (□) reaction between **1** and urea corresponding to the first step of the reaction.

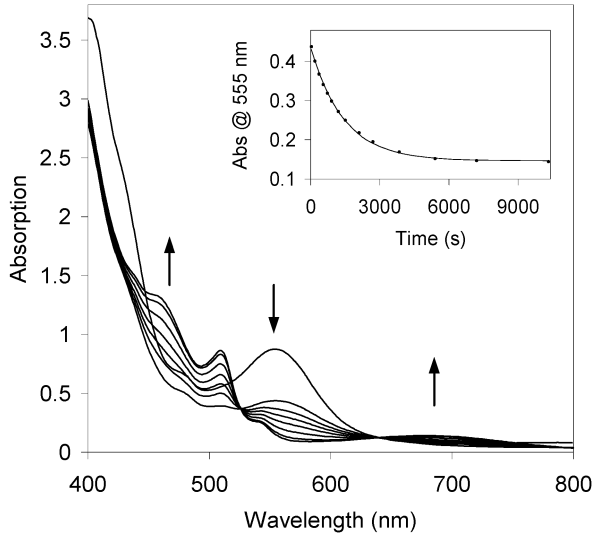

Figure 7. Time-resolved UV−vis spectra for the reaction between **1** and urea acquired using regular UV−vis techniques (1.0 mM of **1** and 16 mM of urea after mixing at 25 °C in acetonitrile). The fast initial drop in absorbance corresponds to the first step of the reaction. The insert shows the kinetic trace at 555 nm, which corresponds to the second step of the reaction fitted to a single-exponential curve.

against acetamide hydrolysis into acetate in the presence of **1**: (1) No ammonia was detected in solutions that were analyzed after the reaction between **1** and acetamide was complete. (2) The formation of a bridged acetamide complex was confirmed by FAB mass spectrometry, with a peak at *m*/*z* 1122.1 corresponding to $\{[Fe_2(\mu\text{-}O)(\mu\text{-}OC(NH)CH_3)(BPMEN)_2](ClO_4)_4\}^-$ in the negative mode and a peak at *m*/*z* 924.2 corresponding to $\{[Fe_2(\mu\text{-}O)(\mu\text{-}OC(NH)CH_3)(BPMEN)_2](ClO_4)_2\}^+$ in the positive mode, with isotopic patterns characteristic of dinuclear iron complexes (peaks at *m*/*z* 1223.0 and 925.2 were observed in control experiments for the acetate analogue **5** under the same experimental conditions).

The reaction between **1** and urea was also followed by NMR. Time-resolved ^{1}H NMR spectra between −20 and 100 ppm were collected over several hours (Figure 8), and the time course of the NMR spectral changes was found to parallel the time evolution of UV−vis spectra. The ^{1}H NMR spectrum of **1** shows peaks paramagnetically shifted over a wide range from −5 to 90 ppm, very similar to the spectrum of complex $[Fe_2(\mu\text{-}O)(\mu\text{-}OH)(BPEEN)_2](ClO_4)_3$ reported by Zheng et al., [24] where BPEEN is *N*,*N*′-diethyl-*N*,*N*′-bis(2-pyridylmethyl)ethane-1,2-diamine, a homologue of BPMEN. Upon addition of urea, new features corresponding to the formation of the ring-closed species **3** appear while the features corresponding to **1** disappear. Immediately after mixing of **1** with urea, a broad signal at ca. 20 ppm grows and then slowly decays in the course of the reaction. The position of this signal is similar to the spectrum of a ring-opened adduct of **1** with 1,3-dimethylurea and to the spectrum of a ring-opened hydrated complex **1a** (Figure S14). These spectral changes, although not very dramatic, may correspond to the ring-opened intermediate **3a**. At the end of the reaction, the spectrum was identical to that obtained by dissolving crystals of a ring-closed product **3** in d_3-acetonitrile, except for the presence of a broader peak at 2.2 ppm due to water released during the reaction.

The ring-closure reaction is slow and was studied using regular UV−vis spectrometry (see Experimental Section). With all urea analogues, the ring-closure step follows a single exponential change of optical absorbance, and the observed rate constant is independent of the concentration of the ligand taken in excess. This supports the hypothesis that the binding of urea or its analogues occurs in the first step and that the ring closure is intramolecular. Table 4 summarizes the rate constants, k_2, determined for this process.

Table 5. Electronic Absorption Spectra in Acetonitrile of Ring-Closed Species with Bridging Ureates, Acetamidate, and Acetate (L = BPMEN)

[LFe(μ-O)(μ-CO(NH)(NH_2))FeL]$^{3+}$ [a]		[LFe(μ-O)(μ-CO(NH)($NHCH_3$))FeL]$^{3+}$ [a]		[LFe(μ-O)(μ-CO(NH)($N(CH_3)_2$))FeL]$^{3+}$ [b]		[LFe(μ-O)(μ-CO(NH)(CH_3))FeL]$^{3+}$ [c]		[LFe(μ-O)(μ-CO(O)(CH_3))FeL]$^{3+}$ [22]	
λ_{max} (nm)	ϵ (M^{-1} cm^{-1})	λ_{max} (nm)	ϵ (M^{-1} cm^{-1})	λ_{max} (nm)	ϵ (M^{-1}.cm^{-1})	λ_{max} (nm)	ϵ (M^{-1} cm^{-1})	λ_{max} (nm)	ϵ (M^{-1} cm^{-1})
437 (sh)	1306	421 (sh)	2831	425	2336	438	1055	422 (sh)	1100
460 (sh)	1145	458 (sh)	2136	455 (sh)	2173	466	1299	464	1310
–	–	–	–	–	–	–	–	495 (sh)	860
509	742	510	1028	509	1034	514	912	512	800
541 (sh)	212	542 (sh)	288	542 (sh)	296	550 (sh)	235	543 (sh)	230
677	123	678	172	673	170	689	152	670	160

[a] Structurally characterized by X-ray diffraction. [b] Isolated as a solid then dissolved in acetonitrile. [c] Generated in situ by mixing **1** with an excess of acetamide.

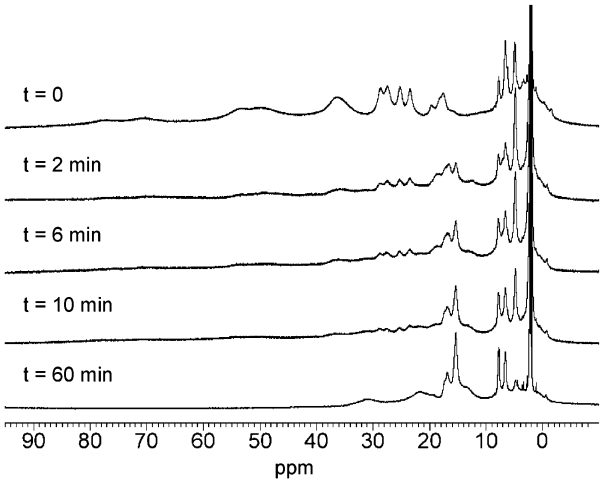

Figure 8. Time resolved ^{1}H NMR spectra for the reaction between **1** and urea (25 mM of **1** and 25 mM of urea after mixing at 25 °C in d_3-acetonitrile).

Experiments on urea hydrolysis were performed with complex **1** and complex **3**. Hydrolysis experiments where ammonia was assayed using the indophenol assay procedure described by Barrios et al.[33] were conducted at different temperatures. No acceleration of ammonia production was observed (see ESI).

Discussion

Our study shows that complex [Fe_2(μ-O)(μ-OH)(BPMEN)$_2$]$^{3+}$ (**1**) in solution easily reacts with a number of ligands, opening the (μ-oxo)(μ-hydroxo)diiron(III) diamond core. The reaction with urea and other amides of the general formula $RCONH_2$ leads eventually to stable complexes [Fe_2(μ-O)(μ-OC(NR_2)NH)(BPMEN)$_2$]$^{3+}$ with N,O-coordinated ureate or amidate ligands. Such reactivity is unusual, especially for ureas, which generally act as monodentate O-ligands.

Deprotonated ureas are uncommon ligands. N-Substituted ureates, like $OC(NR_2)(NR)^-$ and $OC(NR)^{2-}$, were occasionally generated as anionic ligands in organometallic chemistry under strictly anhydrous conditions.[66−69] There is a limited number of structurally characterized nonorganometallic metal complexes with urea anions.[20,70−77] In all of them, deprotonated urea ligands are coordinated through nitrogen (the most basic donor atom), usually as a bridging ligand with μ_2-N,O coordination mode. Neutral ureas, which are much more common ligands, coordinate almost exclusively via the oxygen atom alone[34,78,79] and only rarely form bridges.[80−82] This distinction in the coordination mode also applies to complexes **2**−**4**: the neutral $OC(NH_2)_2$ ligand is monodentately O-coordinated in **2**, while deprotonated ureates form μ_2-N,O bridges in complexes **3** and **4**.

To the best of our knowledge, complex **4** is the first structurally characterized compound with the 1-methylureate anion $CO(NHCH_3)NH^-$. The simple ureate anion $CO(NH_2)$-NH^- present in **3** was only recently structurally characterized, in the μ_2-N,O coordination mode in two dinickel(II) complexes[70,71] and one diiron(III) complex[20] and in the μ_3-N,N′,O mode in a tetranuclear nickel(II) complex.[72] In all those complexes, and also in complex **3** from this work, the ureate $CO(NH_2)NH^-$ anion has similar structural parameters, d(C−O) = 1.24−1.29 Å, d(C−NH) = 1.29−1.31 Å, d(C−NH_2) = 1.37−1.44 Å, and a nearly planar arrangement of all atoms. Although the distinction between the bound oxygen and nitrogen atoms of the ureate molecule is difficult, there is a significant elongation of the distal C−NH_2 bond in the N,O-coordinated ureate compared to the neutral urea [d(C−NH_2) = 1.35 Å],[62] which indicates a partial loss of resonance upon N,O-coordination. The loss of resonance stabilization

(66) Mehrotra, R. C. In *Comprehensive Coordination Chemistry*; Wilkinson, G., Gillard, R. D., McCleverty, J. A., Eds.; Pergamon Press: Oxford, 1987; Vol. 2, pp 269−291.
(67) Cabeza, J. A.; de Rio, I.; Riera, V.; Garcia-Granda, S.; Sanni, S. B. *Organometallics* **1997**, *16*, 3914−3920.
(68) Ruiz, J.; Rodriguez, V.; Vicente, C.; Perez, J.; Lopez, G.; Chaloner, P. A.; Hitchcock, P. B. *Inorg. Chim. Acta* **2003**, *351*, 114−118.
(69) Danopoulos, A. A.; Wilkinson, G.; Sweet, T. K. N.; Hursthouse, M. B. *J. Chem. Soc., Dalton Trans.* **1996**, 3771−3778.
(70) Meyer, F.; Pritzkow, H. *Chem. Commun.* **1998**, 1555−1556.
(71) Buchler, S.; Meyer, F.; Kaifer, E.; Pritzkow, H. *Inorg. Chim. Acta* **2002**, *337*, 371−386.
(72) Meyer, F.; Konrad, M.; Kaifer, E. *Eur. J. Inorg. Chem.* **1999**, 1851.
(73) Fairlie, D. P.; Jackson, W. G.; McLaughlin, G. M. *Inorg. Chem.* **1989**, *28*, 1983−1989.
(74) Cotton, F. A.; Ilsley, W. H.; Kaim, W. *J. Am. Chem. Soc.* **1980**, *102*, 3464−3474.
(75) Thorman, J. L.; Guzei, I. A.; Young, V. G., Jr.; Woo, L. K. *Inorg. Chem.* **1999**, *38*, 3814−3824.
(76) MacBeth, C. E.; Golombek, A. P.; Young, V. G., Jr.; Yang, C.; Kuczera, K.; Hendrich, M. P.; Borovik, A. S. *Science* **2000**, *289*, 938−941.
(77) Gupta, R.; Zhang, Z. H.; Powell, D.; Hendrich, M. P.; Borovik, A. S. *Inorg. Chem.* **2002**, *41*, 5100−5106.
(78) Woon, T. C.; Wickramasinghe, W. A.; Failie, D. P. *Inorg. Chem.* **1993**, *32*, 2190−2194.
(79) Kaminskaia, N. V.; Kostic, N. M. *Inorg. Chem.* **1997**, *36*, 5917−5926.
(80) Barrios, A. M.; Lippard, S. J. *J. Am. Chem. Soc.* **2000**, *122*, 9172−9177.
(81) Mukherjee, S.; Weyhermuller, T.; Bothe, E.; Wieghardt, K.; Chaudhuri, P. *Eur. J. Inorg. Chem.* **2003**, 863−875.
(82) Gentile, P. S.; White, J.; Haddad, S. *Inorg. Chim. Acta* **1974**, *8*, 97−103.

and the elongation of the C−NH_2 bonds is even more pronounced if urea coordinates in the μ-N,O-bridging mode to two metal ions without deprotonation.[82] Such phenomenon may be important in the activation of urea for hydrolysis at the dinuclear nickel(II) core of enzyme urease.[8,20,83]

Even though resonance stabilization of urea is diminished due to its bidentate coordination to the diiron core, no acceleration of urea hydrolysis was observed in complex **3**, in comparison to urea hydrolysis in the absence of this dinuclear complex (see ESI for specific experimental conditions). This behavior can be attributed to a decreased electrophilic character of the carbonyl group in deprotonated urea, which makes the ureate anion less susceptible to nucleophilic attack than a neutral urea molecule.[20,25] Therefore, if the urease enzyme utilizes bidentate urea binding in the catalytic cycle,[8] the hydrogen-bonding network in the enzyme pocket must prevent premature deprotonation of the coordinated substrate.

An alternative hypothesis on the mechanism of urease action suggests monodentate binding of urea to one metal center, followed by a nucleophilic attack by a hydroxide ion bound to the second metal ion in the active site.[84] The ring-opened intermediate **3a** can be considered a close analogue of the reactive intermediate in a monodentate urease mechanism. The intermediate **3a**, with a hydroxide group on one metal and a urea bound through its oxygen on the other, was found to be more stable in the iron(III) BPMEN system than in all of the other kinetically characterized dinuclear complexes reacting with urea.[20,25] However, complex **1**, which rapidly yields **3a** upon reaction with urea, showed no catalytic activity in the hydrolysis of urea. Instead of ammonia generation, coordination of the urea nitrogen to the second metal center, accompanied by the deprotonation of the amide group, dominates the reactivity of **3a**.

In search for reasons of low reactivity of **3a** toward urea hydrolysis, we attempted to determine metric parameters of a monodentate, O-bound urea ligand in its complexes with iron(III) BPMEN system. Unfortunately, we were not able to crystallize **3a** or other intermediates [Fe_2(μ-O)(OH)(L)(BPMEN)](ClO_4)$_3$ (L, urea or urea derivatives). Such iron(III) species with terminal OH^- ligand are sometimes postulated as intermediates in solution[16,18] but apparently tend to oligomerize upon concentration of the solution. The few known examples of solid structurally characterized Fe^{III}−OH complexes have the terminal hydroxy ligand sterically protected and/or strongly hydrogen bonded to other ligands.[24,63,76,85−87] Interestingly, one example of structurally characterized diiron(III) complex containing the (HO)Fe^{III}-(μ-O)Fe^{III}(OH) core has been reported by Fontecave et al.[87]

We were able to isolate and structurally characterize a related mononuclear complex **2**, in which an iron(III) center is surrounded by four nitrogens from BPMEN, one carbonyl oxygen from a neutral, O-bound urea, and one oxygen from an ethoxide group (Figure 2). It is likely that a rather unusual terminal ethoxide in this complex is stabilized by the hydrogen bond between the EtO^- ligand and the NH_2 group of the urea ligand [d(N6−O2) = 2.99 Å, d(H6−O2) = 2.29 Å, angle(N6−H6−O2) = 136.4°], similar to stabilization of a terminal HO^- in urea-appended cavities described by Borovik and co-workers.[76] Analysis of metric parameters of O-bound urea in complex **2** (Table 3) shows that they are similar to the metric parameters of the urea molecule in crystals of pure urea [d(C−O) = 1.26 Å and d(C−N) = 1.35 Å].[62] Therefore, O-coordinated urea in the iron(III) BPMEN system is not strongly activated toward hydrolysis.

Urea, its derivatives, and its analogues have been proven to be sensitive probes in quantitative studies of the reactivity of dinuclear complexes.[20,25] In the present study, a two-step ligand substitution at the (μ-oxo)(μ-hydroxo)diiron(III) core supported by BPMEN ligands was characterized quantitatively. The first, ring-opening step is comparable to a simple reaction of complex **1** with water, which will be discussed first.

Complex **1** is known to undergo partial hydration to form **1a**.[23] From our kinetic data (Table 4), the equilibrium constant, at 25 °C, was determined to be K_1= 1.8 M^{-1}. This value is lower than, but of the same magnitude as, the one previously reported by Poussereau et al. using regular spectroscopic titration at an unspecified (apparently room) temperature (K_1= 5.4 M^{-1}).[23] In our hands, the determination of the equilibrium constant by analysis of UV−vis spectra gave K_1= 2.9 M^{-1} at 25 °C. The enthalpy and entropy changes for this process are $\Delta H°$ = −29 kJ mol^{-1} and $\Delta S°$ = −93 J mol^{-1} K^{-1} (Table 4). The reaction is driven by the favorable enthalpy due to bond formation, and the value of $\Delta S°$ is typical for a ligand-binding process. The activation entropy for water binding to **1** is negative (−43 J mol^{-1} K^{-1}), indicative of an associative process. The reverse reaction, water dissociation from **1a**, has a positive activation entropy (49.7 J mol^{-1} K^{-1}) characteristic of a dissociative rate-limiting step.

The proposed mechanism of urea binding using the diiron BPMEN complex [Fe_2(μ-O)(μ-OH)(BPMEN)$_2$](ClO_4)$_3$ (**1**) (Scheme 3) is a two-step process, the first step corresponding to the addition of urea followed by the second step, elimination of a molecule of water and binding of the deprotonated urea nitrogen. This mechanism is similar to one proposed for the formation of the acetate-bridged BPMEN diiron complex **5**.[22] Previous kinetic investigations of urea binding to dimetal complexes have been performed starting with the diiron(III) complex of TPA[20] and the pyrazolate-based dinickel(II) complex of L^{pyz} (Scheme 1).[25] A major difference in these three systems is that **1** has a diamond core structure, Fe(μ-O)(μ-OH)Fe, whereas complexes of TPA and L^{pyz} are present in the hydrate form (H_2O)M(μ-O)M-

(83) Maslak, P.; Sczepanski, J. J.; Parvez, M. *J. Am. Chem. Soc.* **1991**, *113*, 1062−1063.
(84) Karplus, P. A.; Pearson, M. A.; Hausinger, R. P. *Acc. Chem. Res.* **1997**, *30*, 330−337.
(85) Yeh, C.-Y.; Chang, C. J.; Nocera, D. G. *J. Am. Chem. Soc.* **2001**, *123*, 1513−1514.
(86) Ogo, S.; Wada, S.; Watanabe, Y.; Iwase, M.; Wada, A.; Harata, M.; Jitsukawa, K.; Masuda, H.; Einaga, H. *Angew. Chem., Int. Ed.* **1998**, *37*, 2102−2104.
(87) Duboc-Toia, C.; Ménage, S.; Vincent, J.-M.; Averbuch-Pouchot, M. T.; Fontecave, M. *Inorg. Chem.* **1997**, *36*, 6148−6149.

Table 6. Comparison of Rate Constants and Equilibrium Constants for Urea Binding to Dinuclear Metal Complexes at 25 °C in Acetonitrile[a]

starting complex	$[Fe_2(\mu\text{-}O)(\mu\text{-}OH)(BPMEN)_2]^{3+}$	$[Fe_2(\mu\text{-}O)(OH)(OH_2)(TPA)_2]^{3+}$ [20]	$[Ni_2(\mu\text{-}O)(OH)(OH_2)(L^{pyz})]^{2+}$ [25]
first step k_1 (M^{-1} s^{-1})	5.9 ± 0.2	$>10^5$	$>10^5$ [b]
preequilibrium K_1	37 ± 2	9 ± 3	0.29[b]
second step k_{2obs} (s^{-1})	$(6.6 \pm 0.6) \times 10^{-4}$	2.6	0.39[b]
overall K	600 ± 70	650 ± 100	2.7(5)

[a] The structures of the ligands are shown in Scheme 1. [b] In acetone.

(OH) and $(H_2O)M(\mu\text{-}L^{pyz})M(OH)$, respectively. Selected rate and equilibrium constants are compared in Table 6.

The reaction of **1** with urea is slow (several hours) as compared to the reaction with the TPA analogue, which occurs within seconds. The same trend in reactivity between the BPMEN system and the TPA system has been reported in the acetate substitution reaction.[22] Such labilization of the iron(III) complexes of TPA may be attributed to the kinetic trans-influence of a stronger donor atom (pyridine nitrogen) in the equatorial position, where the analogous BPMEN complexes contain a much weaker donor (tertiary aliphatic nitrogen). However, the overall equilibrium constant (see ESI for the calculation) is essentially the same in both cases (Table 6), indicating the absence of the thermodynamic trans-effect. In the presence of water, lower rate constants were observed for the ring-closure step ($k_2 = 4.2 \times 10^{-4}$ s^{-1} in the presence of excess of water). The reaction is also expected to be base-sensitive. The acid−base effects in ligand substitution deserve a separate detailed investigation and were not a subject of this study.

All substituted ureas investigated in this study also reacted with complex **1**. 1-Methylurea and 1,1-dimethylurea follow the two-step mechanism as described for urea. The preequilibrium constants ($K_1 = 33$ and 37 M^{-1}, respectively) are comparable to that of urea ($K_1 = 37$ M^{-1}) and much larger than the one obtained with water ($K_1 = 1.8$ M^{-1}) (Table 4). The rate constants for the forward and reverse reactions are of similar values with all substituted ureas in the first binding step ($k_1 = 3.2-6.7$ M^{-1} s^{-1} and $k_{-1} = 0.095-0.183$ s^{-1} at 25 °C) (Table 4). However, the second step rate constant was observed to decrease as the number of methyl groups on the nonbinding nitrogen increased [k_2(urea) = 6.6 s^{-1}, k_2(1-methylurea) = 1.2 s^{-1} and k_2(1,1-dimethylurea) = 0.5 s^{-1}] (Table 4). The presence of methyl groups on both nitrogens inhibits this process, apparently due to steric hindrance. The binding of 1,3-dimethylurea is similar to the first binding process observed with urea. However, the rate constant of the forward reaction is significantly smaller ($k_1 = 1.5$ M^{-1} s^{-1} at 25 °C) than that of urea and resembles in value the rate constant obtained with water ($k_1 = 1.8$ M^{-1} s^{-1} at 25 °C). The equilibrium constant is significantly lower for 1,3-dimethylurea ($K_1 = 9.9$ M^{-1}) than for urea ($K_1 = 37$ M^{-1}). The reaction with tetramethylurea was found to be more complex than that observed with other ureas. As in the reaction with water, the equilibrium constant is much lower than with other substituted ureas ($K_1 = 1.2$ M^{-1}). The kinetics of the first reaction between **1** and tetramethylurea, which could only be followed at very high concentrations of the ligand (ca. 85−140 mM) could not be described by the simple model depicted for urea and other substituted ureas. Although we could not determine the individual rate constants for ligand binding and dissociation in this case, it was clear that the reaction is slower than analogous processes with less sterically bulky ligands.

Acetamide reacted with **1** in a two-step mechanism similar to the one observed with urea. The rate constant for the ring-closure step with acetamide is 60-fold smaller than that with urea, with k_2(acetamide) = 0.11×10^{-4} s^{-1}. This can be explained by the difference in acidity between urea (with pK_a in water about 14)[88] and acetamide (with pK_a in water about 15).[89,90] Preliminary results regarding the ring-closure step for the formation of the acetate complex **5** by mixing **1** and acetic acid confirmed the hypothesis that more acidic protons on the incoming group favor the ring-closure process [k_2(acetic acid) = 5×10^{-2} s^{-1}].

The published data on kinetics of ligand substitution in dinuclear iron complexes are rather limited.[16,17,20] It has been shown that terminal ligands at diiron centers undergo rapid substitution in one observable step with the rates similar to ligand exchange in mononuclear iron(III) complexes.[17] Similarly, substitution of a terminal water molecule for an O-bonded urea in the complex $[Fe_2(\mu\text{-}O)(OH)(OH_2)(TPA)_2]^{3+}$ occurred rapidly (the reaction was too fast to be followed by the stopped-flow methodology at room temperature).[20] In contrast, substitution of a bridging acetate for a bridging dihydrophosphate in dinuclear iron(III) complexes with triaza macrocycles was found to be several orders of magnitude slower.[16] The observed reaction step had a zero order in the incoming ligand, in agreement with a rate-limiting solvolytic (hydrolytic in aqueous media) acetate ring opening. The ensuing steps, including the substitution of a monodentate acetate for a monodentate dihydrophosphate, followed by the phosphate ring closure, were proposed to be rapid.[16]

The reactions of complex **1**, outlined in Scheme 3, are the first examples of ligand substitution at a (μ-oxo)(μ-hydroxo)diiron(III) diamond core that were studied in detail by kinetic methods. In the first reaction step, the hydroxo-bridge opens up, and the new ligand coordinates, in a monodentate fashion, to one iron(III) center. In the second reaction step, which only occurs with sterically unhindered amides, the second ligating group of the incoming ligand binds to the second iron(III) center, thus closing the ring. The rate of oxo-bridged ring opening depends on both the concentration and the nature of the incoming ligand. It

(88) Blakeley, R. L.; Treston, A.; Andrews, R. K.; Zerner, B. *J. Am. Chem. Soc.* **1982**, *104*, 612−614.
(89) Branch, G. E. K.; Clayton, J. O. *J. Am. Chem. Soc.* **1928**, *50*, 1680−1686.
(90) Baush, M. J.; David, B.; Dobrowolski, P.; Guadalupe-Fasano, C.; Gostowski, R.; Selmarten, D.; Prasad, V.; Vaughn, A.; Wang, L.-H. *J. Org. Chem.* **1991**, *56*, 5643−5651.

appears that the hydration of **1**, with the formation of **1a**, does not facilitate coordination of urea or its analogues. The ligand binding rate constant, k_1, is faster for urea than it is for water. Furthermore, addition of several different urea analogues occur with different k_1 values, some of which are greater than k_1 for hydration, while the others (e.g., 1,1,3,3-tetramethylurea) are slower than hydration. The first step of ligand addition to an oxo−hydroxo core in **1** is characterized by negative activation entropies indicative of associative processes. Taken together, the results suggest a nucleophilic attack by the incoming ligand at one of the iron(III) centers as a rate-limiting step in the ring-opening process. The on rates (k_1) decrease as the number of methyl substituents on the incoming urea ligand increases, while the off rates (k_{-1}) somewhat increase for more bulky ureas. This results in lower binding affinity of complex **1** for substituted urea derivatives. The relatively weak binding of water is related to a faster water dissociaton rate from the complex **1a** as compared to urea dissociation from **3a**, in agreement with a weaker Fe−(OH_2) bond as compared to the Fe−$OC(NH_2)_2$ bond. As expected for a ligand dissociation process, the activation entropies are positive (Table 4). The second reaction step, ring closure due to coordination of the second functional group of the incoming ligand to the second iron(III) center, is highly sensitive to steric effects and is also sensitive to the pK_a of the incoming bidentate ligand. This is an intramolecular process that requires the presence of at least one unsubstituted NH_2 group in the amide functionality of the incoming ligand.

Conclusions

The kinetic and thermodynamic studies of the hydroxo-bridge substitution in the (μ-oxo)(μ-hydroxo)diiron(III) core are reported for the first time, using reactions of the complex [Fe_2(μ-O)(μ-OH)(BPMEN)$_2$](ClO_4)$_3$ (**1**) with water, urea, and a series of urea derivatives and analogues as incoming ligands. The reaction of **1** with $RC(O)NH_2$ occurs in two distinct, observable steps: diamond core ring-opening with concomitant monodentate coordination of the incoming ligand, followed by the closure of a six-membered ring, yielding stable complexes with bidentate, deprotonated amidates, [Fe_2(μ-O)(μ-OC(R)NH)(BPMEN)$_2$]$^{3+}$. The first reaction step, O-coordination of the incoming ligand, is an associative process. The equilibrium and rate constants of this reaction decreased upon addition of methyl groups on both nitrogens of urea. The second reaction step is even more sensitive to steric effects: the bidentate N,O-coordination was observed with urea, 1-methylurea, 1,1-dimethylurea, and acetamide, but not with 1,3-dimethyl- and 1,1,3,3,-tetramethylurea. The rate constants for the ring closure are also sensitive to the acidity of the leaving proton. The reaction products with urea and 1-methylurea were structurally characterized. An elongation of the C−NH_2 bond in the N,O-coordinated ureate compared to neutral urea was observed. However, metric parameters of the O-bonded urea in a related complex [Fe(BPMEN)(urea)(EtO)](ClO_4)$_2$ (**2**) were close to the metric parameters of pure crystalline urea. Bidentate N,O-coordination of urea is more effective than its monodentate coordination through the oxygen atom in disrupting resonance stabilization of the urea molecule.

Acknowledgment. The authors thank Dr. Richard J. Staples (Harvard University), Prof. Terry E. Haas (Tufts University), and Prof. Alexander Y. Nazarenko (SUNY College at Buffalo), for helpful discussions on crystallography issues, and Dr. David J. Wilbur (Tufts University), for his assistance with the instrumentation methods, in particular electrospray mass spectrometry. This work was supported by the NSF (CHE 0111202). The CCD-based X-ray diffractometer at Tufts University was purchased through Air Force DURIP grant F49620-01-1-0242. The NMR facility in the Chemistry Department at Tufts University was supported by NSF grant CHE 9723772, and the ESI mass spectrometer was funded by the NSF grant MRI 0320783.

Supporting Information Available: Electronic spectra of complexes **1** and **1a**, electrospray mass spectra of the reaction mixture of **1** with 1,1-dimethylurea, detailed concentration and temperature dependencies of the ligand binding rates, ^{1}H NMR spectra, details of equilibrium studies, experiments on urea hydrolysis, and crystallographic details for the complexes **1**−**4**. This material is available free of charge via the Internet at http://pubs.acs.org.

IC049371X